

Harvesting Excitons through Plasmonic Strong Coupling

Carlos Gonzalez-Ballester¹, Johannes Feist¹, Esteban Moreno¹, and Francisco J. Garcia-Vidal^{1,2}

¹*Departamento de Física Teórica de la Materia Condensada and Condensed Matter Physics Center (IFIMAC), Universidad Autónoma de Madrid, E-28049 Madrid, Spain*

²*Donostia International Physics Center (DIPC), E-20018 Donostia/San Sebastian, Spain*

Exciton harvesting is demonstrated in an ensemble of quantum emitters coupled to localized surface plasmons. When the interaction between emitters and the dipole mode of a metallic nanosphere reaches the strong coupling regime, the exciton conductance is greatly increased. The spatial map of the conductance matches the plasmon field intensity profile, which indicates that transport properties can be tuned by adequately tailoring the field of the plasmonic resonance. Under strong coupling, we find that pure dephasing can have detrimental or beneficial effects on the conductance, depending on the effective number of participating emitters. Finally, we show that the exciton transport in the strong coupling regime occurs on an ultrafast timescale given by the inverse Rabi splitting (~ 10 fs), orders of magnitude faster than transport through direct hopping between the emitters.

PACS numbers: 71.35.-y, 05.60.Gg, 73.20.Mf, 81.05.Fb

Bound electron-hole pairs in semiconductors and molecular solids, known as excitons, play a key role in many basic processes such as Förster resonance energy transfer or energy conversion in light-harvesting complexes [1–3]. Various optoelectronic devices are also based on exciton dynamics, including organic solar cells [4], light-emitting diodes [5], and excitonic transistors [6]. Thus, a large research effort is directed towards controlling exciton transport properties. As excitons usually suffer from relatively large propagation losses associated with decoherence and recombination, increasing their propagation length is an important goal. Moreover, the transport of these quasiparticles into a specific spatial region in a controlled way could significantly increase the efficiency of devices such as solar cells, where the presence of excitons close to the charge separation region is essential for photocurrent generation.

Recent works [7, 8] have shown that exciton conductance in an ensemble of organic molecules can be boosted by several orders of magnitude when the ensemble is coupled to a cavity mode and the system enters the strong coupling (SC) regime. This is a promising result, which motivates the exploration of this phenomenon beyond cavity setups. Among the fields in which the SC regime is very attractive, plasmonics stands out due to the recent works studying SC between surface plasmons and quantum emitters (QEs) [3, 9–12, 14–20]. Surface plasmons arise as ideal platforms for SC applications, due to their small mode volume and the tunability of their electric field profile via nanostructure design. These characteristics could allow for a deterministic control of exciton harvesting.

In this Letter we demonstrate efficient harvesting of excitons in a collection of QEs strongly coupled to localized surface plasmons (LSPs). As a proof of principle, we first study a system of QEs interacting with the dipolar modes supported by a metal nanosphere (NS). We show how within the SC regime the spatial map of the exciton conductance mirrors the field intensity profile. Employing a structure composed of three aligned nanospheres, we show that the ef-

iciency of exciton harvesting can be significantly increased by tuning the electric field profile of the LSP mode. In addition, we demonstrate that the role of dephasing in the exciton conductance strongly depends on the effective number of emitters involved in the formation of the polariton modes. Finally, we demonstrate that the speed of exciton transport in the SC regime is orders of magnitude faster than in the weak coupling regime.

The first system we consider consists of a silver NS of radius R , surrounded by a layer of N QEs, as shown in Fig. 1a. For simplicity, the QEs are regularly distributed over a spherical layer, which we place at a distance $h = 1$ nm away from the surface of the NS. Note that at this short distance, higher multipole modes of the NS are dominant and lead to quenching losses for a single QE [21]. However, recent works have shown that for N emitters, collective SC with the dipole resonance of the NS does indeed arise, and higher multipoles merely add an effective detuning to the hybrid mode [18]. Hence, for the silver nanosphere we only consider the three dipolar LSP modes (x, y, z) , which are characterized by their frequency ω_{pl} and decay rate κ , and electric field profile $\vec{E}_\alpha(\vec{r})$ ($\alpha \in x, y, z$). These parameters can be extracted from the NS properties, as described in the Supplemental Material [22]. The QEs are modelled as point dipoles oriented along the radial direction, with transition frequency ω_0 , dipole moment $\vec{\mu}$, and total decoherence rate $\gamma = \gamma_\phi + \gamma_d$, where γ_ϕ accounts for pure dephasing, while the decay rate $\gamma_d = \gamma_r + \gamma_{nr}$ contains radiative and nonradiative contributions.

The Hamiltonian associated with the emitters-NS system within the rotating wave approximation can be written as

$$H = \sum_j \omega_0 c_j^\dagger c_j + \sum_{\alpha=x,y,z} \omega_{pl} a_\alpha^\dagger a_\alpha + \sum_{i \neq j} V_{ij} (c_i^\dagger c_j + H.c.) + \sum_{j,\alpha} (g_{j\alpha} c_j^\dagger a_\alpha + H.c.). \quad (1)$$

Here, the operators c_j and a_α annihilate an excitation in emitter j ($= 1, \dots, N$) and the LSP mode α , respectively.

The dipole-dipole interaction between QEs is given by V_{ij} , and the QE-LSP coupling is $g_{j\alpha} = -\vec{\mu} \cdot \vec{E}_\alpha(\vec{r}_j)$. As we will show later, in the SC regime only a single LSP mode contributes and dipole-dipole interactions can be neglected. Under these approximations and for zero detuning ($\omega_0 = \omega_{pl}$), the $N + 1$ singly excited eigenstates of H are formed by: i) two polaritons $|\pm\rangle = \frac{1}{\sqrt{2}}(a^\dagger|0\rangle \pm |B\rangle)$, where $|B\rangle = \frac{2}{\Omega_R} \sum_i g_i c_i^\dagger |0\rangle$ is the collective molecular bright state, with Ω_R the Rabi splitting ($\Omega_R^2 = 4 \sum_j |g_j|^2$), and ii) the so-called dark states, $N - 1$ combinations of molecular excitations orthogonal to $|B\rangle$ which have no LSP component. The eigenfrequencies of the two polaritons are $\omega_0 \pm \Omega_R/2$.

In order to study exciton transport through the ensemble of emitters, we first determine the steady state of the system when one of the QEs (emitter A from now on) is incoherently pumped. Notice that this is the only driving term and no additional external illumination is present. The system is described by its density operator ρ , whose dynamics is governed by the master equation $\dot{\rho} = -i[H, \rho] + \sum_j \gamma \mathcal{L}_{c_j} + \sum_\alpha \kappa \mathcal{L}_{a_\alpha} + \gamma_p \mathcal{L}_{c_A^\dagger}$. Incoherent processes (losses and pump) are described by Lindblad terms, $\mathcal{L}_b[\rho] = b\rho b^\dagger - \{b^\dagger b, \rho\}/2$. In the first part of this work we treat pure dephasing as a decay channel for simplicity. The pumping rate γ_p is chosen small enough to stay in the linear regime. The steady state density matrix ρ_{ss} is obtained numerically using the open-source QuTiP package [23]. Finally, the exciton conductance measuring the efficiency of exciton transfer from emitter A to emitter j is calculated as $\sigma_e^{(j)} = J_{(A \rightarrow j)}/\gamma_p$, where $J_{(A \rightarrow j)} = \gamma \text{Tr}(H \mathcal{L}_{c_j}[\rho_{ss}])$ is the energy loss rate of emitter j [7].

The exciton conductance is shown in Fig. 1b for QEs at three representative positions, B , C , and D , as depicted in Fig. 1a. With organic molecule applications in mind, the parameters of the $N = 100$ QEs are chosen to correspond to TDBC J-aggregates at room temperature [24–26]: $\omega_0 = 2.11$ eV, $\mu = 0.749$ e-nm, $\gamma_\phi = 26.3$ meV, $\gamma_r = 1.32 \cdot 10^{-6}$ eV, $\gamma_{nr} = 1.10$ meV. The nanosphere (radius $R = 10$ nm) is embedded in a dielectric host of permittivity $\epsilon_d = 6.8$, so that the LSPs are in resonance with the QEs. Finally, the plasmon losses are given by $\kappa = 0.1$ eV. In order to study different Rabi frequencies Ω_R , we first artificially tune the field strength of the LSPs, instead of varying the number of QEs as could be done experimentally. Our results show how the onset of SC clearly differentiates two different regimes for exciton transport. In the weak coupling case (small Ω_R), the dipole-dipole interaction between the QEs governs the dynamics and the transport is rather inefficient over large distances. The exciton conductance to emitter D is thus smaller than that to B or C . In the SC regime, however, this situation changes drastically, as LSP-mediated interaction becomes the primary transport channel [7]. Due to the dipolar field profiles, emitter A only couples to the z -dipole mode of the NS, and the x and y dipole play a

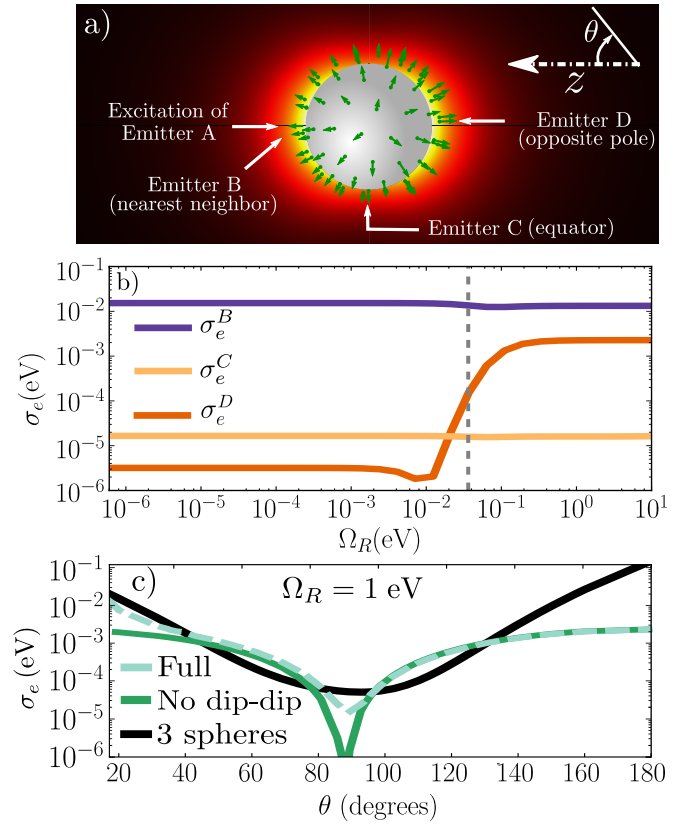


FIG. 1. (color online) a) Illustration of the single-NS system. The colored background shows the electric field intensity associated with the z -oriented dipole mode. b) Exciton conductance versus Rabi splitting for $N = 100$ emitters. The gray dashed line indicates the onset of SC, $\Omega_R \gtrsim |\gamma - \kappa|/2$. c) Angular dependence of the conductance in the SC regime (light green) and the same quantity when neglecting dipole-dipole interaction between QEs (dark green). For comparison the three-NS case is also depicted (black line).

negligible part. As the couplings $g_{j\alpha}$ are proportional to the electric field of mode α , excitons are transferred more efficiently to regions of high field intensity. This is the cause of the boost in the conductance of emitter D displayed in Fig. 1b.

These results indicate that the strong coupling conductance is position-dependent, mimicking the field intensity profile. This fact is confirmed in Fig. 1c. Here, we plot the conductance in the SC regime for every QE versus its polar angular coordinate θ . The results without dipole-dipole coupling ($V_{ij} = 0$) agree very well with the full calculation. The significant dip of σ_e around $\theta = 90^\circ$ confirms that only the z -oriented LSP mode plays a relevant role. Therefore, we can safely neglect both the dipole-dipole interactions and the x - and y -oriented LSP modes within the SC regime. Under these approximations, an analytical solution for the master equation can be obtained [22]. For zero detuning ($\omega_{pl} = \omega_0$), the exciton conductance between emitters A

and j has the simple form

$$\sigma_e^{(j)} = \frac{16|g_A|^2|g_j|^2\omega_0(\gamma + \Gamma)}{\Gamma(\Omega_R^2 + \gamma\kappa)(\Omega_R^2 + 2\gamma\Gamma)}, \quad (2)$$

where we have defined the rate $\Gamma = \gamma + \kappa$, and $g_j \equiv g_{jz}$ for simplicity. Up to now, we have considered the case in which both the pumping and collection involve a single QE, and Ω_R is artificially modified by tuning the field strength of the LSP while keeping N constant. In a realistic experiment, several emitters near location A would be pumped, and excitons collected from a region around D . Furthermore, $\Omega_R \propto \sqrt{N}$ would be varied by changing the number of emitters N . Equation (2) is easily generalized to this case, giving

$$\sigma_e = \frac{\eta_A\eta_D\omega_0(\gamma + \Gamma)\Omega_R^4}{\Gamma(\Omega_R^2 + \gamma\kappa)(\Omega_R^2 + 2\gamma\Gamma)}, \quad (3)$$

where $\eta_X = 4\sum_{j \in X}|g_j|^2/\Omega_R^2$ measures the fraction of the Rabi frequency due to emitters involved in the pumping (η_A) and collection processes (η_D), respectively. Both η_A and η_D are independent of N for uniform distributions of emitters. For small N (i.e., weak coupling), Eq. (3) shows that σ_e grows as N^2 , while when the SC regime is entered for large N ($\Omega_R^2 \gg \gamma\Gamma$), it saturates to a constant value, $\eta_A\eta_D\omega_0(1 + \gamma/\Gamma)$. This equation thus predicts that the exciton transport efficiency from a pumping site to a collection spot can be increased by tailoring the mode to have maximal field strength at (only) these two locations in order to have large η_A and η_D .

We demonstrate this by adding two additional identical silver nanospheres to the existing structure, as shown in Fig. 2a. The background of the panel displays the field intensity map of the lowest energy mode, which in this case is not degenerate as the rotational symmetry is broken. The spheres are separated by a 2 nm gap. In order to facilitate the comparison with the single-NS case and focus on the effect of the different mode profile, the LSP frequency and losses as well as the QE properties and locations are kept unchanged. Furthermore, we again plot the single-emitter to single-emitter conductance. The exciton conductance as a function of the Rabi splitting is displayed in Fig. 2b for $N = 100$. As the figure shows, the onset of SC again produces a substantial increase in the pole-to-pole conductance σ_e^D , significantly larger than in the single-NS case. The most striking feature of this system is that transport to emitter D is now much more efficient than to the nearest neighbor B of emitter A . The conductance in the SC regime is much more concentrated around the poles than in the single-NS (see Fig. 1c), and conductance to point D is increased by a factor of 50. Excitons are thus shown to be very efficiently harvested at the *hot spots* of the LSP mode. This is an interesting result towards potential applications, due to the high tunability provided by the wide variety of plasmonic nanostructures that are available nowadays.

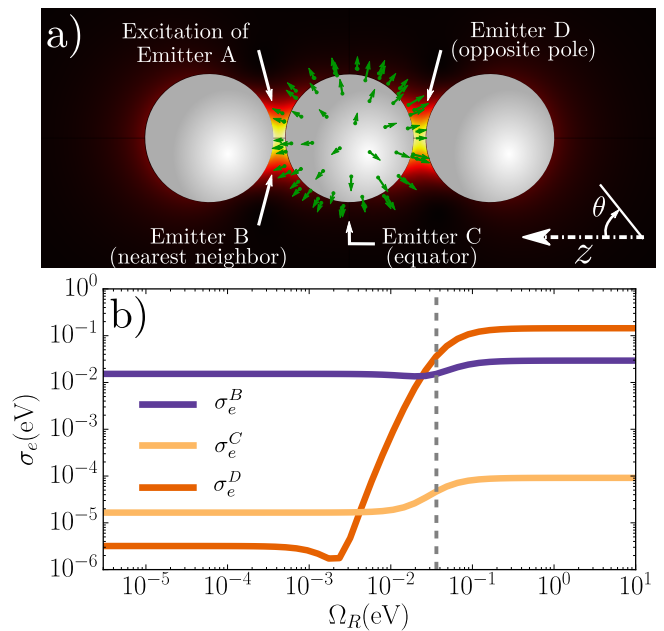


FIG. 2. (color online) a) Illustration of the three-NS system. The colored background shows the electric field intensity of the lowest energy mode. b) Exciton conductance versus Rabi splitting for $N = 100$ emitters. The curves correspond to transport from emitter A to emitters B , C , and D as depicted in panel (a). As in Fig. 1b, the gray dashed line indicates the onset of SC.

Up to now, our treatment of relaxation processes has been relatively crude, lumping together dissipation and dephasing. Recent works show that dephasing mechanisms can be relevant for exciton transport in organic compounds [2]. Therefore, we now describe pure dephasing in more detail by performing the substitution $\gamma\mathcal{L}_{c_j} \rightarrow \gamma_d\mathcal{L}_{c_j} + \gamma_\phi\mathcal{L}_{c_j^\dagger c_j}$ in the master equation. In order to avoid unrealistic conclusions, we have also checked that the complementary Bloch-Redfield-Wangsness formalism [27] reproduces the general behavior obtained with the standard Lindblad method.

The pole-to-pole exciton conductance in the SC regime is shown in Fig. 3 as a function of the dephasing rate, for both the single-NS and the three-NS cases. Except for the value of γ_ϕ , the parameters of the three nanospheres and the QEs are the same as in the previous calculations. Surprisingly, the dependence of the conductance with dephasing is remarkably different for the two considered nanostructures. As dephasing is increased, the conductance decreases monotonically for the three-NS structure, but counterintuitively increases for the single NS. As we show next, this difference in behavior is related to the effective number of QEs that enter strong coupling with the LSP. This number is quite small in the three-NS case, where only QEs near the hot spots participate in SC. Our hypothesis is confirmed by considering a system of N non-interacting QEs uniformly coupled to a cavity mode ($g_j = g$). In this simple situation, an analytical formula for the exciton conductance can be

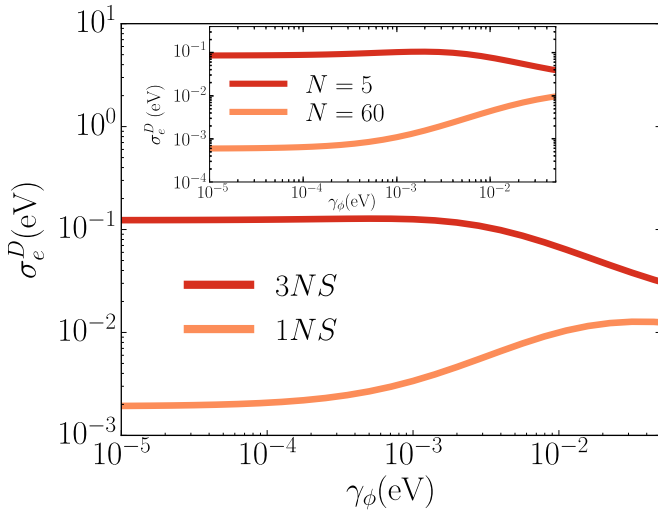


FIG. 3. Exciton conductance from point *A* to point *D* in the SC regime ($\Omega_R = 1$ eV), as a function of the dephasing rate. The single-NS case (orange line) is compared with the three-NS structure (red line). The inset displays the conductance in the SC regime for a system of QEs uniformly coupled to the field, in the cases $N = 5$ and $N = 60$.

derived [7], which in the SC limit is given by

$$\sigma_e = \frac{\omega_0 \gamma_d (\gamma_d + \gamma_\phi) (\kappa + 2\gamma_d + 2\gamma_\phi)}{(2\gamma_\phi + \gamma_d N) (\kappa \gamma_\phi + \gamma_d N (\kappa + \gamma_d + \gamma_\phi))}. \quad (4)$$

This simple expression (shown in the inset of Fig. 3) is able to reproduce the observed features. Specifically, the ratio $\sigma_e(\gamma_\phi \rightarrow \infty) / \sigma_e(\gamma_\phi \rightarrow 0)$ is approximately equal to $\gamma_d N^2 / \kappa$. Since typical plasmonic structures fulfill $\gamma_d / \kappa \ll 1$, this expression predicts that with increasing dephasing, exciton conductance decreases for small N ($N < \sqrt{\kappa / \gamma_d}$), but increases for sufficiently large N ($N > \sqrt{\kappa / \gamma_d}$). This dependence with the number of emitters suggests that the dark states play a key role in this process. Since dephasing creates an incoherent coupling between the dark modes and the polaritons, a fraction of the population in the dark modes can be transferred to the polaritons. For large N , the dark states are highly populated as the overlap between the initial state (one excitation at emitter *A*) and the polaritons is extremely small. As a consequence, the excitation transfer to the polaritons can compensate for the detrimental effect of dephasing on this state, making the conductance increase.

While we have so far focused on the conductance as obtained in the steady state under pumping, the temporal dynamics of the system provides important additional insight. We thus investigate the population dynamics in the single NS case, for an initial excitation of emitter *A*. In the weak coupling regime, the dipole-dipole interaction dominates and slowly transfers population to emitter *D* (as shown in Fig. 4a). The plasmon modes do not significantly participate in the dynamics, so that all populations decay with the lifetime of the bare QEs ($\tau \sim 600$ fs) for large times. As the exciton transport is even slower, the increase of population

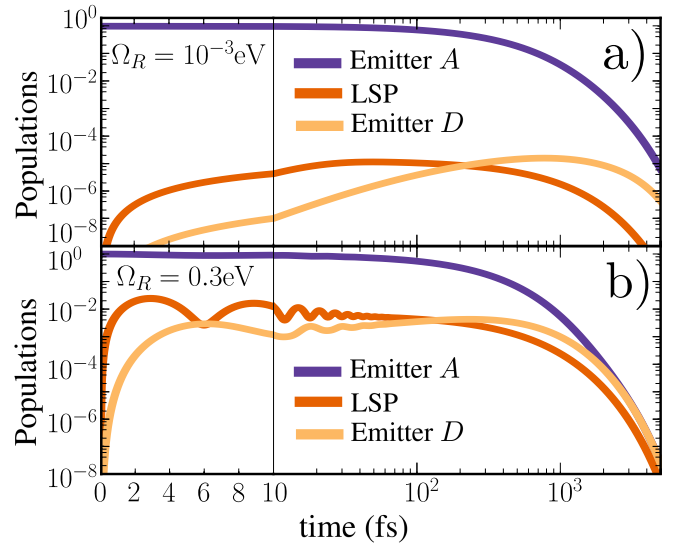


FIG. 4. (color online). Time dynamics of the single NS system when QE *A* is initially excited (initial state $c_A^\dagger |0\rangle$) and no pump is applied. The populations of both the main LSP and the relevant emitters, *A* and *D*, are displayed as a function of time. a) Weak coupling case, $\Omega_R = 10^{-3}$ eV. b) Strong coupling case, $\Omega_R = 0.3$ eV. In both panels, the linear scale for short times allows for a better visualization of the results.

in emitter *D* is cut off at around this time, with a maximum population of $\sim 2 \cdot 10^{-5}$. On the other hand, in the SC regime (Fig. 4b), the population is delivered to the emitter *D* much more efficiently through Rabi oscillations. These proceed on a timescale determined by the inverse of the Rabi splitting ($1/\Omega_R \sim 15$ fs in Fig. 4b), giving extremely fast population transfer. Furthermore, the population of emitter *D* reaches significantly larger values than in the weak coupling regime, up to $\sim 4 \cdot 10^{-3}$. For large times, most of the population is trapped in the dark states, which can now also decay through the dephasing-induced coupling to the polaritons, giving an effective lifetime somewhat below the bare QEs.

In conclusion, we have demonstrated the feasibility of harvesting excitons through strong coupling in systems composed of a plasmonic structure and an ensemble of organic molecules. We have shown that for emitters coupled to the localized surface plasmons of a single nanoparticle, the exciton conductance map mimics the electric field profile of the plasmon resonance. Taking advantage of this property, we have devised a more complex structure in which an exciton can be efficiently transferred between two subwavelength hot-spots of the plasmonic system. We have also shown how dephasing can be beneficial or detrimental depending on the number of emitters that are effectively coupled to the plasmon resonance. We have additionally demonstrated that exciton transport in the strong coupling regime proceeds orders of magnitude faster than under weak coupling. Finally, it is worth noting that our findings regarding harvesting of excitons mediated by strong coupling are general and appli-

cable to any quantum emitter, from atoms and quantum dots to organic molecules, and also to any confined electromagnetic mode with similar properties as the plasmonic ones used here.

This work has been funded by the European Research Council (ERC-2011-AdG Proposal No. 290981), the Spanish MINECO (FPU13/01225 fellowship and MAT2011-28581-C02-01 grant), and by the European Union Seventh Framework Programme under grant agreement FP7-PEOPLE-2013-CIG-618229.

-
- [1] Gregory S. Engel, Tessa R. Calhoun, Elizabeth L. Read, Tae-Kyu Ahn, Tomas Mancal, Yuan-Chung Cheng, Robert E. Blankenship, and Graham R. Fleming, "Evidence for wave-like energy transfer through quantum coherence in photosynthetic systems," *Nature* **446**, 782 (2007).
- [2] F. Caruso, A. W. Chin, A. Datta, S. F. Huelga, and M. B. Plenio, "Highly efficient energy excitation transfer in light-harvesting complexes: The fundamental role of noise-assisted transport," *J. Chem. Phys.* **131**, 105106 (2009).
- [3] Gregory D. Scholes, Graham R. Fleming, Alexandra Olaya-Castro, and Rienk van Grondelle, "Lessons from nature about solar light harvesting," *Nat. Chem.* **3**, 763 (2011).
- [4] S. Matthew Menke, Wade A. Luhman, and Russell J. Holmes, "Tailored exciton diffusion in organic photovoltaic cells for enhanced power conversion efficiency," *Nat. Mater.* **12**, 152 (2013).
- [5] Simone Hofmann, Thomas C. Rosenow, Malte C. Gather, Björn Lüssem, and Karl Leo, "Singlet exciton diffusion length in organic light-emitting diodes," *Phys. Rev. B* **85**, 245209 (2012).
- [6] Alex A. High, Ekaterina E. Novitskaya, Leonid V. Butov, Micah Hanson, and Arthur C. Gossard, "Control of exciton fluxes in an excitonic integrated circuit," *Science* **321**, 229 (2008).
- [7] Johannes Feist and Francisco J. Garcia-Vidal, "Extraordinary exciton transport mediated by strong coupling," *Phys. Rev. Lett.*, (in press) (2014), [arXiv:1409.2514](https://arxiv.org/abs/1409.2514).
- [8] Johannes Schachenmayer, Claudiu Genes, Edoardo Tignone, and Guido Pupillo, "Cavity enhanced transport of excitons," (2014), [arXiv:1409.2550](https://arxiv.org/abs/1409.2550).
- [9] J. Bellessa, C. Bonnand, J. C. Pleniet, and J. Mugnier, "Strong coupling between surface plasmons and excitons in an organic semiconductor," *Phys. Rev. Lett.* **93**, 036404 (2004).
- [10] Y. Sugawara, T. A. Kelf, J. J. Baumberg, M. E. Abdelsalam, and P. N. Bartlett, "Strong coupling between localized plasmons and organic excitons in metal nanovoids," *Phys. Rev. Lett.* **97**, 266808 (2006).
- [11] Nche T. Fofang, Tae-Ho Park, Oara Neumann, Nikolay A. Mirin, Peter Nordlander, and Naomi J. Halas, "Plexcitonic nanoparticles: Plasmon-exciton coupling in nanoshell-J-aggregate complexes," *Nano Lett.* **8**, 3481 (2008).
- [12] Andreas Trügler and Ulrich Hohenester, "Strong coupling between a metallic nanoparticle and a single molecule," *Phys. Rev. B* **77**, 115403 (2008).
- [3] Edo Waks and Deepak Sridharan, "Cavity QED treatment of interactions between a metal nanoparticle and a dipole emitter," *Phys. Rev. A* **82**, 043845 (2010).
- [14] T. Schwartz, J. A. Hutchison, C. Genet, and T. W. Ebbesen, "Reversible switching of ultrastrong light-molecule coupling," *Phys. Rev. Lett.* **106**, 196405 (2011).
- [15] C. Van Vlack, Philip Trøst Kristensen, and S. Hughes, "Spontaneous emission spectra and quantum light-matter interactions from a strongly coupled quantum dot metal-nanoparticle system," *Phys. Rev. B* **85**, 075303 (2012).
- [16] A. González-Tudela, P. A. Huidobro, L. Martín-Moreno, C. Tejedor, and F. J. García-Vidal, "Theory of strong coupling between quantum emitters and propagating surface plasmons," *Phys. Rev. Lett.* **110**, 126801 (2013).
- [17] Andrea E. Schlather, Nicolas Large, Alexander S. Urban, Peter Nordlander, and Naomi J. Halas, "Near-field mediated plexcitonic coupling and giant rabi splitting in individual metallic dimers," *Nano Lett.* **13**, 3281 (2013).
- [18] A. Delga, J. Feist, J. Bravo-Abad, and F. J. Garcia-Vidal, "Quantum emitters near a metal nanoparticle: Strong coupling and quenching," *Phys. Rev. Lett.* **112**, 253601 (2014).
- [19] P. Törmä and W. L. Barnes, "Strong coupling between surface plasmon polaritons and emitters: a review," *Rep. Prog. Phys.* **78**, 013901 (2015).
- [20] Gülis Zengin, Martin Wersäll, Sara Nilsson, Tomasz J. Antosiewicz, Mikael Käll, and Timur Shegai, "Realizing strong light-matter interactions between single nanoparticle plasmons and molecular excitons at ambient conditions," *Phys. Rev. Lett.* **114**, 157401 (2015).
- [21] Pascal Anger, Palash Bharadwaj, and Lukas Novotny, "Enhancement and quenching of single-molecule fluorescence," *Phys. Rev. Lett.* **96**, 113002 (2006).
- [22] See Supplemental Material at URL for more details on the calculation of the mode properties, quantization of the LSP fields and derivation of an analytical formula for the exciton conductance.
- [23] J. R. Johansson, P. D. Nation, and Franco Nori, "QuTiP 2: A python framework for the dynamics of open quantum systems," *Comp. Phys. Comm.* **184**, 1234 (2013).
- [24] Johannes Moll, Siegfried Daehne, James R. Durrant, and Douwe A. Wiersma, "Optical dynamics of excitons in J-aggregates of a carbocyanine dye," *J. Chem. Phys.* **102**, 6362 (1995).
- [25] Stéphanie Valleau, Semion K. Saikin, Man-Hong Yung, and Alán Aspuru Guzik, "Exciton transport in thin-film cyanine dye J-aggregates," *J. Chem. Phys.* **137**, 034109 (2012).
- [26] Tal Schwartz, James A. Hutchison, Jérémie Léonard, Cyrille Genet, Stefan Haacke, and Thomas W. Ebbesen, "Polariton dynamics under strong lightmolecule coupling," *ChemPhysChem* **14**, 125 (2013).
- [27] Heinz-Peter Breuer and Francesco Petruccione, *The theory of open quantum systems* (Oxford University Press, 2002)

Supplemental Material

CALCULATION OF THE MODE PROPERTIES

We calculate the classical field profiles and modal characteristics of the localized surface plasmon (LSP) numerically with the finite element method (using COMSOL Multiphysics) to solve Maxwell's equations. The permittivity of the silver structures is given by a Drude-Lorentz formula:

$$\epsilon(\omega) = \epsilon_\infty - \frac{\omega_p^2}{\omega(\omega + i\gamma_D)} - \Delta \frac{\Omega_P^2}{\omega^2 - \Omega_P^2 + i\omega\Gamma_P}, \quad (1)$$

where the parameters $\epsilon_\infty = 3.91$, $\omega_p = 8.833$ eV, $\gamma_D = 0.0553$ eV, $\Delta = 0.76$, $\Omega_P = 4.522$ eV, and $\Gamma_P = 8.12$ eV are taken from Ref. [1]. For the dipole mode of the single NS, we obtain a frequency $\omega_{pl} = 2.11$ eV and a dissipation rate $\kappa = 0.12$ eV. In the three-NS structure, the parameters of the lowest energy mode are $\omega'_{pl} = 1.85$ eV, and $\kappa' = 0.14$ eV. Note that in the main text these values are modified artificially to agree with the single-NS case, in order to isolate the influence of the electric field profile.

QUANTIZATION OF LSP FIELDS

The classical fields of the system modes obtained from Maxwell's equations have to be properly quantized in order to include them in a quantum Hamiltonian. In this section we briefly detail the method followed for this purpose.

Single-sphere case

The dipole mode of a single sphere is quantized by comparing the classical and quantum values of the polarizability α . For a small metallic sphere of permittivity $\epsilon(\omega)$ and radius R , the classical static polarizability is given by [?]]

$$\alpha_{cl} = 4\pi\epsilon_0\epsilon_d R^3 \frac{\epsilon(\omega) - \epsilon_d}{\epsilon(\omega) + 2\epsilon_d}, \quad (2)$$

being ϵ_d the permittivity of the surrounding dielectric. For simplicity, we introduce an approximate Drude permittivity (Eq. (1), with $\Delta = 0$). We can define a resonance frequency $\omega_r = \omega_p/\sqrt{\epsilon_\infty + 2\epsilon_d}$ and, after some algebra [3], arrive to the following expression:

$$\alpha_{cl} \approx -2\pi\epsilon_0\epsilon_d R^3 \frac{3\epsilon_d}{\epsilon_\infty + 2\epsilon_d} \frac{\omega_r^2}{\omega(\omega - \omega_r + i\gamma_D/2)}, \quad (3)$$

which is valid in the vicinity of a narrow resonance, i.e. $\omega \approx \omega_r \ll \gamma_D$.

On the other hand, the polarizability of a quantum two-level system with dipole moment μ is given by [4]:

$$\alpha_q = \frac{\mu^2}{\hbar} \frac{2\omega_0}{\omega_0^2 - (\omega + i\gamma_0/2)^2}, \quad (4)$$

where ω_0 and γ are the two-level system frequency and linewidth, respectively. Close to a narrow resonance ($\omega \approx \omega_0 \ll \gamma_0$), the above expression is approximated as

$$\alpha_q \approx -\frac{\mu^2}{\hbar} \frac{\omega_0}{\omega(\omega - \omega_0 + i\gamma_0/2)}. \quad (5)$$

By direct comparison of Eqs. (3) and (5), we obtain the dipole moment of a nanosphere in a quantum model:

$$\mu_{pl} = \left(\hbar\omega_{pl} \frac{6\pi\epsilon_0\epsilon_d^2 R^3}{\epsilon_\infty + 2\epsilon_d} \right)^{1/2}. \quad (6)$$

The quantum electric field in this case corresponds to the classical field emitted by a dipole with dipole moment μ_{pl} .

Arbitrary geometry

For more complex nanostructures, the eigenmodes do not possess a purely dipolar profile, and a new quantization procedure is necessary. We start with the classical electric and magnetic field profiles obtained from our simulations, $\vec{E}_{cl}(\vec{r})$ and $\vec{H}_{cl}(\vec{r})$. We generalize the usual quantization procedure for vacuum fields [4], by applying the correspondence principle to the electromagnetic energy:

$$U(\vec{E}_{cl}, \vec{H}_{cl}) \leftrightarrow H(\vec{E}_q, \vec{H}_q). \quad (7)$$

In the above expression, U stands for the total classical electromagnetic energy, and H for the Hamiltonian operator. The quantum field operators \vec{E}_q, \vec{H}_q are related to their classical counterparts,

$$\begin{aligned} \vec{E}_q &= C\vec{E}_{cl}a + C^*\vec{E}_{cl}^*a^\dagger, \\ \vec{H}_q &= C\vec{H}_{cl}a + C^*\vec{H}_{cl}^*a^\dagger, \end{aligned} \quad (8)$$

where a and a^\dagger are the photonic mode annihilation and creation operators, respectively, and C is a normalization constant we have to determine.

Our systems are composed of a metallic nanostructure surrounded by a dielectric host, with permittivities $\epsilon(\omega)$ and ϵ_d respectively. Usually, the electromagnetic energy U is ill-defined in lossy media, and a macroscopic QED formalism is required. However, in the vicinity of a narrow resonance $\omega = \omega'_{pl}$, and provided that the losses are small ($\text{Im}[\epsilon(\omega)] \ll \text{Re}[\epsilon(\omega)]$), the following approximation holds [5]

$$\begin{aligned} U &\approx \frac{\epsilon_0}{2} \int_{V_{\text{metal}}} dV \text{Re} \left[\frac{d(\omega\epsilon(\omega))}{d\omega} \right]_{\omega=\omega'_{pl}} \vec{E}_{cl}^* \cdot \vec{E}_{cl} \\ &+ \frac{\epsilon_0\epsilon_d}{2} \int_{V_{\text{diel}}} dV \vec{E}_{cl}^* \cdot \vec{E}_{cl} + \frac{\mu_0}{2} \int_{V_{\text{tot}}} dV \vec{H}_{cl}^* \cdot \vec{H}_{cl}. \end{aligned} \quad (9)$$

We apply the correspondence principle, Eq. (7), by introducing the quantum fields (8) in the above equation, i.e. substituting $(\vec{E}_{cl}^*, \vec{E}_{cl}, \vec{H}_{cl}^*, \vec{H}_{cl})$ by $(\vec{E}_q^\dagger, \vec{E}_q, \vec{H}_q^\dagger, \vec{H}_q)$. After manipulation, we arrive to the familiar Hamiltonian

$$H = |C|^2 U (2a^\dagger a + 1). \quad (10)$$

The comparison with the Hamiltonian of a harmonic oscillator, $H = \hbar\omega'_{pl}(a^\dagger a + 1/2)$, gives the expression of the normalization constant,

$$C = \sqrt{\frac{\hbar\omega'_{pl}}{2U}}. \quad (11)$$

Finally, after C is determined, the calculation of the couplings $g'_j = -\vec{\mu} \cdot C \cdot \vec{E}_{cl}(\vec{r}_j)$ is straightforward.

It is important to mention that, when calculating the energy U from our simulations, we have to deal with the linear divergence of the second integral in Eq. (9). This is a fundamental problem regarding lossy cavities, in which normal modes are ill-defined. In our case, we can safely ignore the divergent contribution due to the low loss rate [6]. The validity of this approximation has been checked in the single nanosphere case, where this method reproduces the analytical results obtained above very accurately.

ANALYTICAL FORMULA FOR THE CONDUCTANCE

Here we give details of the calculation of the formula for the conductance (Eq. (2) in the main text). In the absence of dipole-dipole interaction, and considering only one of the dipole modes, the Hamiltonian of the system is given by the

Tavis-Cummings expression,

$$H = \omega_0 \sum_{j=1}^N c_j^\dagger c_j + \omega_{pl} a^\dagger a + \sum_j (g_j a^\dagger c_j + \text{H.c.}). \quad (12)$$

It is useful to work in the bright-dark basis, which is composed of a bright state $|B\rangle$,

$$|B\rangle = \frac{2}{\Omega_R} \sum_{j=1}^N g_j c_j^\dagger |0\rangle, \quad (13)$$

and a set of $(N - 1)$ dark states. In principle, we are free to choose any orthonormal set of states, and we use this freedom to our advantage. As in our problem we pump the first molecule (state $c_1^\dagger |0\rangle$), we choose the dark states such that this pumping only excites one of them, which we name $|D\rangle$. It is straightforward to prove that

$$|D\rangle = \frac{2g_1}{G'\Omega_R} \left(\frac{G'^2}{g_1^*} c_1^\dagger - \sum_{j=2}^N g_j c_j^\dagger \right) |0\rangle, \quad (14)$$

where we have defined $G'^2 = (\Omega_R/2)^2 - g_1^2$ for simplicity. The remaining dark states $\{|D_k\rangle; k = 1, \dots, N - 2\}$ are arbitrary, provided that they fulfill the orthogonality conditions $\langle D_k | B \rangle = \langle D_k | D \rangle = 0$. Note that Eqs. (13) and (14) imply that $\langle D_k | \sigma_1^\dagger | 0 \rangle = \langle D_k | (a | B \rangle + b | D \rangle) = 0$.

Consequently, the states $\langle D_k |$ are not coupled to the pumped state and do not take part in the dynamics. The time evolution of the system is thus restricted to the 4-dimensional subspace spanned by the states $\{|0\rangle, |B\rangle, |D\rangle, a^\dagger |0\rangle\}$, and the master equation reduces to a 16×16 linear system.

We can thus calculate the steady-state density matrix analytically, from which it is straightforward to obtain the exciton conductance. With the notation employed in the main text, the general expression is given by

$$\sigma_e(j) = -16|g_j|^2 |g_A|^2 \frac{\gamma \delta (\kappa \Omega_R^2 + 4\gamma \Gamma^2) + \omega_0 (\Omega_R^2 \Gamma (\Gamma + \gamma) - 2\gamma (2\gamma^3 + 5\kappa \gamma^2 - 4\delta^2 \kappa + 4\gamma \kappa^2 + \kappa^3))}{(-\Omega_R^4 + 4\gamma (4\delta^2 + \Gamma^2)) (\Omega_R^2 \Gamma^2 + \gamma \kappa (4\delta^2 + \Gamma^2))}, \quad (15)$$

where we have defined the detuning $\delta = \omega_{sp} - \omega_0$. The case of zero detuning $\delta \rightarrow 0$ reduces the above expression to Eq. (2) in the main text.

-
- [1] Zhiming M Wang, ed., *One-dimensional nanostructures* (Springer New York, 2008).
 [2] Craig F. Bohren and Donald R. Huffman, *Absorption and*

scattering of light by small particles (Wiley-VCH, 2008).

- [3] Edo Waks and Deepak Sridharan, "Cavity QED treatment of interactions between a metal nanoparticle and a dipole emitter," *Phys. Rev. A* **82**, 043845 (2010).
 [4] Rodney Loudon, *The quantum theory of light* (Oxford University Press, 2000).
 [5] Stefan Alexander Maier, *Plasmonics: fundamentals and applications* (Springer US, 2007).
 [6] A. F. Koenderink, "On the use of Purcell factors for plasmon antennas," *Opt. Lett.* **35**, 4208–4210 (2010).